

Experiment and Dynamic Simulations of Radiation Damping of Laser-polarized liquid ^{129}Xe at low magnetic field in a flow system

Xin Zhou*, Jun Luo, Xian-ping Sun, Xi-zhi Zeng,

Ming-sheng Zhan, Shang-wu Ding, Mai-li Liu

State Key Laboratory of Magnetic Resonance and Atomic and Molecular Physics,

Wuhan Institute of Physics and Mathematics,

The Chinese Academy of Sciences, P. O. Box 71010,

Wuhan 430071, People's Republic of China

Abstract

Radiation damping is generally observed when the sample with high spin concentration and high gyro-magnetic ratio is placed in a high magnetic field. However, we firstly observed liquid state ^{129}Xe radiation damping using laser-enhanced nuclear polarization at low magnetic field in a flow system in which the polarization enhancement factor for the liquid state ^{129}Xe was estimated to be 5000, and furthermore theoretically simulated the envelopes of the ^{129}Xe FID and spectral lineshape in the presence of both relaxation and radiation damping with different pulse flip angles and ratios of T_2^*/T_{rd} . The radiation damping time constant T_{rd} of 5 ms was derived based on the simulations. The reasons of depolarization and the further possible improvements were also discussed.

* Corresponding author. E-mail: xinzhou@wipm.ac.cn; Tel: +86-27-8719-7796; Fax: +86-27-8719-9291.

I. INTRODUCTION

Laser-polarized ^{129}Xe and ^3He gases [1] have been found wide applications in polarized targets [2], magnetic resonance imaging (MRI) [3, 4], neutron polarization [5], fundamental symmetry studies [6], high resolution nuclear magnetic resonance (NMR) spectroscopy [7], surface science [8], precision measurements [9], biological-system probe [10], quantum computer [11] and cross polarization to other nuclei [12, 13]. The enhanced NMR signals of laser-polarized ^{129}Xe , which are about 10^5 times larger than those from thermally polarized ^{129}Xe [1, 14], have opened the possibility to explore radiation damping effect [15] of laser-polarized ^{129}Xe .

Since Bloembergen and Pound analyzed the physical process of radiation damping in 1954 [15], radiation damping had been noticed and studied in the early time [16, 17, 18, 19]. Although the research of radiation damping in NMR had almost halted from 1960 to 1988, it has once again evoked the interest of researchers in recent years because of the applications of high field magnets and high sensitive probes. Since then, a large number of research articles and reviews have been published [20, 21, 22, 23, 24, 25, 26, 27, 28, 29].

Radiation damping is a non-linear effect. The current, induced by the transverse magnetization in the receiver rf coil, interacts with the magnetization vector itself, tending to bring it back to the $+Z$ axis (the direction of the static magnetic field). Radiation damping is usually observed at high fields where liquid phase magnetization M , the static magnetic field homogeneity, and the quality factor Q of the probe are high enough [15, 16, 20]. The magnetization is $M=\gamma\hbar CP$ in the light of the Currie law, with γ the gyromagnetic ratio, P the polarization, and C the spin concentration. In aqueous solutions the water proton concentration is usually 110 mol/L ($C\approx 110$ M), which is high enough to produce radiation damping effect. Radiation damping can also be observed for other solvents and concentrated samples [30]. According to the thermal-polarization $P_0(B_0, T)\approx \gamma h B_0 / (4\pi k T)$, either decreasing the temperature or increasing the magnetic field can enhance the polarization and make radiation damping effect stronger, but it can provide only limited relief. It's very natural to employ optical pumping and spin exchange [1] to improve the polarization.

Although radiation damping of laser-polarized gaseous xenon was obtained at 14 T on Bruker DRX 600 spectrometer [31], the proper inversion of the magnetization could not be entirely interpreted with the dipolar field theory [32]. The dipolar field effects [33], on

the other hand, could explain NMR instabilities and spectral clustering in laser-polarized liquid xenon [34]. In medical MRI, the existence of radiation damping both in the phantom experiments and in vivo affects the quality of imaging [35], and one can foresee that the same problem will emerge in application of the lung MRI using hyperpolarized ^3He and ^{129}Xe [3]. Therefore, until now, the microcosmic mechanism of radiation damping have be still not fully understood, and the corresponding dynamics problems need to be resolved.

Two recent articles [36, 37] have reported radiation damping of laser-polarized ^3He , which is easier to be observed than that of ^{129}Xe because the gyromagnetic ratio γ and optical pumping efficiency of ^3He is larger than that of ^{129}Xe . Here we report first observation of radiation damping in laser-polarized liquid ^{129}Xe at the low magnetic field in a flow system, and the typical radiation damped FID envelopes and spectra at different pulse flip angles are presented and compared with theoretical ones. Characterization of such a system is important for hyperpolarized MRI at low magnetic fields [38]. Our experiment could provide another liquid phase example to analysis radiation damping effect. In addition, laser-polarized liquid xenon and its radiation damping also have a number of potential applications, such as construction of liquid xenon maser [39], rapid and precise measurement of liquid xenon polarization [40], etc..

II. EXPERIMENT

The diagram of our experimental apparatus is shown in Figure 1. The pump cell containing a few drops of metal Cs was maintained at approximately 333 ± 1 K by the resistance heater during optical pumping. The inner surfaces of the cylindrical Pyrex tube and the pump cell were coated with silane in order to slow down the relaxation of the ^{129}Xe upon collision with the tube wall. The cell was placed in a 25 Gauss magnetic field generated by Helmholtz coils. The whole system was evacuated with K2 valve close and K1, K3 and K4 valves open. When the vacuum reached 1.5×10^{-5} Torr, the valves K1, K4 were closed and K2, K3 were opened. The cell was filled with 740 Torr natural xenon gas (26% enriched ^{129}Xe gas). After all the valves were closed, laser light from a 15 W laser array (Opto Power Co. Model OPC-D015-850-FCPS) at 852.1 nm was introduced to the system. The laser light resonates with the Cs D_2 transition line and induces an electron spin polarization in the Cs vapor via a standard optical pumping process [41]. The hyperpolarized ^{129}Xe gas

was produced by spin-exchange collision at the same time. The polarization process took about 25 minutes. K4 valve was then opened to allow the ^{129}Xe to be transmitted into the probe, pre-cooled to 172 ± 1 K, of Bruker SY-80M NMR spectrometer. The temperature of the probe was, subsequently, reduced to 160 ± 1 K to freeze the xenon into condensed state. But the actual temperature, which was somewhat different from the monitor's, was improved from NMR observation that solid phase and liquid phase xenon co-exist in the probe because the temperature rang between the melting point and the boiling point of xenon was small (4.6 ± 3 °C). To study radiation damping of the liquid ^{129}Xe , the sample was cooled down to 142 ± 1 K to completely freeze the xenon, and then gradually warmed up and maintained at 166 ± 1 K.

III. RESULTS AND DISCUSSION

Figure 2 shows the ^{129}Xe NMR time domain signal (a) and the corresponding spectrum (b) at the temperature of 160 ± 1 K when 160° pulse was applied. The peak with larger line width at high frequency ($\delta 147$) is assigned to solid ^{129}Xe and the sharp peak with phase distortion ($\delta 108$) is from liquid ^{129}Xe (Fig. 2b). Such phase distortion is the typical result of the radiation damping.

It should be noted that at the temperature of 166 ± 1 K, only liquid state ^{129}Xe NMR signal at $\delta 108$ is observable. Figure 3 shows the ^{129}Xe FID signals (a1-a4) and the corresponding frequency spectra (b1-b4) excited by 60° , 90° , 120° , and 150° pulses, respectively. Compared with the water theoretical FID envelope and spectrum in Figure 4 [17, 23], these signals obviously indicated that the laser-polarized liquid ^{129}Xe have radiation damping effects. Unlike conventional FID (Fig. 3 a1-a2), the profile of typical radiation damped FID excited by a pulse flip angle greater than 90° will increase initially, and start to decay after reaching a maximum, and the position of the maximum is flip angle dependent (Fig. 3 a3-a4). As it is expected, the amplitude of symmetrical phase twisting of the corresponding spectra is enhanced when the flip angle is increased (Fig. 3 b3-b4) [24, 25].

The strength of radiation damping is characterized by radiation damping time constant T_{rd} [16]. The longitudinal relaxation time (T_1) of ^{129}Xe in liquid phase is about 30 minutes [42, 43]. The T_2^* of ^{129}Xe in the NMR machine (Bruker SY-80M) due to the poor inhomogeneity is estimated to be 30 ms. Radiation damping can occur only when T_{rd} is shorter

than T_2^* [24]. Compared with T_2^* and T_{rd} , T_1 effect is negligible. The value of T_{rd} can be estimated from the line-width of spectrum obtained by using very small pulse flip angle, since in this case the line shape will be reduced to a Lorentzian [25].

$$\Delta v_{1/2} = q/\pi T_2^* = \pi^{-1}[(1/T_2^*) + (1/T_{rd})] \quad (1)$$

Considering the error of $\Delta v_{1/2}$ and T_2^* , the values of T_{rd} was in the range of 6 ± 2 ms. Then, according to the analytical results of the Bloch equations including only T_{rd} and T_2^* , which have been presented in the Mao's paper [25],

$$S(\omega) = (2M_0 T_{rd} q / T_2^*) \sum (-1)^n \frac{(2n+1)q/T_2^*}{[(2n+1)q/T_2^*]^2 + \omega^2} [\tan(\eta/2)]^{2n+1}, (for : 0 < \eta \leq \pi/2); \quad (2)$$

$$(2M_0 T_{rd} q / T_2^*) \sum (-1)^n \frac{(2n+1)q/T_2^*}{[(2n+1)q/T_2^*]^2 + \omega^2} \{2 \cos(\omega t_0) - [\cot(\eta/2)]^{2n+1}\}, (for : \pi/2 < \eta \leq \pi). \quad (3)$$

with

$$q = [1 + (T_2^*/T_{rd})^2 + 2(T_2^*/T_{rd}) \cos \theta_0]^{1/2}, \quad (4)$$

$$t_0 = -(T_2^*/q) \tanh^{-1} \{[(T_2^*/T_{rd}) \cos \theta_0 + 1]/q\}, \quad (5)$$

$$\cos \eta = [(T_2^*/T_{rd}) \cos \theta_0 + 1]/q, \quad (6)$$

we simulated the spectra with different T_{rd} values and pulse flip angles in order to get the accurate T_{rd} value. And the same simulation of the FID was performed using the formula [25]:

$$M_y = (M_0 T_{rd} / T_2^*) q \sec h[(q/T_2^*)(t - t_0)]. \quad (7)$$

T_2^* of liquid state ^{129}Xe was assumed to be 30 ms in all simulations unless otherwise indicated, which was the same as the experimental one. As a result, we found the precise T_{rd} of laser-polarized liquid ^{129}Xe was about 5ms in our experiment. The simulated ^{129}Xe FID and corresponding frequency spectrum, assumed the 150° pulse and $T_{rd}=5$ ms, are respectively visualized in Figure 5 (a) and (b), which are in good agreement with our experimental results [Fig. 3 (a4) and (b4)].

Figure 6 shows the theoretically simulated envelopes of the ^{129}Xe FID in the presence of relaxation and radiation damping with different flip angle pulses and T_{rd} values. From the spectra, we can learn that the envelope of the FID is associated with the ratio of T_2^*/T_{rd} and the flip angle θ_0 . If $T_2^*/T_{rd} \leq 1$, the bigger the ratio is, the faster the FID decays when $\theta_0 \leq 90^\circ$, contrary to the cases of $\theta_0 > 90^\circ$; and the radiation damping impossibly occurs and the maximum amplitude point is located at $t=0$ whatever the flip angle θ_0 is. If $T_2^*/T_{rd} > 1$, the same situation occurs that the bigger the ratio is, the faster the FID decays; but when $\theta_0 > 90^\circ$ the FID grows up at first, then falls down after reaching the maximum amplitude point, which is higher when the ratio is bigger. The spectra also indicate that the FID decays monotonically when $\theta_0 \leq 90^\circ$ no matter what the ratio is. The radiation damping can be observed only when $T_2^*/T_{rd} > 1$ and when the pulse flip angle is greater than 90° . The bigger T_2^*/T_{rd} is, the stronger radiation damping will be. The radiation damping will also occur even when $T_2^*/T_{rd}=2$. So our observation of the liquid ^{129}Xe radiation damping under the conditions of the large ^{129}Xe magnetization and the ratio of $T_2^*(30\text{ms})/T_{rd}(5\text{ms})=6$ is reasonable.

Based upon the relation of the magnetization versus the nuclear spin polarization given by Abragam [19], and by comparison of the nuclear spin polarization P_L of ^{129}Xe produced by laser optical pumping with the Boltzmann polarization P_B of ^{129}Xe at the thermal equilibrium, the enhancement factor of the ^{129}Xe nuclear spin polarization can be expressed as:

$$f = \frac{P_L}{P_B} = \frac{I_L}{I_B} \quad (8)$$

where I_L and I_B are the integral intensities of the measured NMR signals of the liquid ^{129}Xe under the conditions of the laser optical pumping and the thermal equilibrium, respectively. Therefore, the enhancement factor of the liquid ^{129}Xe was about 5000 on the basis of our measurement [44]. The Boltzmann polarization P_B of the ^{129}Xe at 166 K in the Bruker SY-80M (1.879 Tesla) spectrometer is about 2.9×10^{-6} , hence the liquid state ^{129}Xe nuclear spin polarization P_L is 1.45%, which was produced by spin exchange with laser-polarized Cs atoms at the low magnetic field of 25 Gauss in a flow system.

From the qualitative face, radiation damping emerges when the transverse relaxation time T_2^* is longer than the characteristic time of radiation damping $T_{rd} = \frac{1}{2\pi\eta Q M \gamma}$ [15, 16, 20], although the quality factors Q of our Bruker SY-80M NMR spectrometer is rather poor and the filling factor is rather small, and the radiation damping effect is about four times

more efficient in the case of protons than for ^{129}Xe nuclei at the same magnetization level because of the dependence of T_{rd} on the gyromagnetic ratio. But when the ^{129}Xe nuclear polarization is enhanced, the signal intensity of liquid ^{129}Xe is larger than that of water protons in a high magnetic field by comparing water protons signals at 11.7 Telsa and room temperature ($C=110$ M, $P=4.2\times 10^{-5}$, $M=7.83\times 10^{-5}$ G/cm³) with laser-polarized liquid ^{129}Xe signals ($C=5.46$ M, $P=1.45\times 10^{-2}$, $M=3.69\times 10^{-4}$ G/cm³). The value of T_2^* will dramatically be shortened due to the magnetic field inhomogeneity, so radiation damping of water protons could not be observed on the same SY-80M spectrometer, but with the enhancement of polarization, we have observed the liquid phase radiation damping for our laser-polarized sample. The phenomenon, that radiation damping occurs for liquid ^{129}Xe but not for solid ^{129}Xe under the same polarization condition, also demonstrates that radiation damping depends primarily on both the intensity of the magnetization and the characteristic time of radiation damping T_{rd} .

The polarization in a flow system is not so high as that in the close pump cell or produced by the narrow bandwidth Ti:Sapphire laser [31]. The main causes are: (a) The loss of polarization is due to the magnetic field inhomogeneity during the transfer of laser-polarized ^{129}Xe gases. (b) Since the bandwidth of our diode laser array is 30 \AA but the absorbed bandwidth of Cs atom in the 740 Torr natural xenon is only 30 GHz, the efficient pump power is only about 0.125 W. (c) The phase transition of laser-polarized ^{129}Xe can also bring about the depolarization. (d) The relaxation of ^{129}Xe atoms at the walls still decreases the polarization even though they were coated.

Thus we can see the further possible improvements in our experiment by adopting the following techniques: (a) Creating the homogeneous magnetic field by two-layer solenoid with end correction coils, and keeping the transmission of laser-polarized xenon paralleling the static magnetic field. (b) Increasing the gas pressure of the pump cell in order to enhance the optical-pumped absorbed power. (c) Decreasing the time of phase transition of laser-polarized ^{129}Xe .

IV. CONCLUSIONS

Usually radiation damping was observed only when the sample has high spin concentration, such as water protons, in the high magnetic field with high-resolution spectrometer.

However, our experiment indicated that under the condition of laser-enhanced nuclear polarization, which made the liquid ^{129}Xe polarization enhancement of 5000 compared to that without optical pumping under the same conditions, the liquid ^{129}Xe radiation damping can also be observed even at low magnetic field in a flow system. The liquid ^{129}Xe T_{rd} of our experiment was estimated to be as short as 5ms with the help of radiation damping line shape theory, and we theoretically simulated the FID and spectrum of ^{129}Xe in the presence of radiation damping and the transverse relaxation in order to compare with the experimental ones. We also discussed whether the radiation damping would occur with different ratios of T_2^*/T_{rd} , and the theoretically simulated envelopes of the ^{129}Xe FID in the presence of both relaxation and radiation damping with different pulse flip angles and T_{rd} values were presented. The reasons of depolarization and the further possible improvements were also discussed. Furthermore, our experiment of laser-polarized liquid ^{129}Xe NMR may be a partially good test bed for studying micro-mechanism of radiation damping.

V. ACKNOWLEDGMENTS

This work is supported by the National Natural Science Foundation of China under Grant No. 10234070, National Science Fund for Distinguished Young Scholars under Grant No. 29915515 and National Fundamental Research Program under Grant No. 2001CB309306. One of the author (X. Z.) is grateful to Dr. Xi-an Mao for helpful discussions and suggestions.

-
- [1] Walker T. G. and Happer W.: Phys. Rev. Lett. **69**, 629-642 (1997).
 - [2] Xu W. *et al.*: Phys. Rev. Lett. **85**, 2900-2904 (2000).
 - [3] Albert M. S., Cates G. D., Driehuys B., Happer W., Saam B., Springer C. S. Jr and Wishnia A.: Nature **370**, 199-201 (1994).
 - [4] Eberle B., Weiler N., Markstaller K., Kauczor H. -U., Deninger A., Ebert M., Grossmann T., Heil W., Lauer L. O., Roberts T. P. L., Schreiber W. G., Surkau R., Dick W. F., Otten E. W. and Thelen M.: J. Appl. Physiol. **87**, 2043-2052 (1999).
 - [5] Jones G. L, Gentile T. R., Thompson A. K., Chowdhuri Z., Dewey M. S., Snow W. M. and Wietfeldt F. E.: Nucl. Instrum. Methods Phys. Res. Sect. A **440**, 772-776 (2000).

- [6] Rosenberry M. A. and Chupp T. E.: Phys. Rev. Lett. **86**, 22-25 (2000).
- [7] Raftery D., Long H., Meersmann T., Grandinetti P. J., Reven L. and Pines A.: Phys. Rev. Lett. **66**, 584-587 (1991).
- [8] Pietrass T., Bifone A. and Pines A.: Surf. Sci. **334**, L730-L734 (1995).
- [9] Bear D., Stoner R. E., Walsworth R. L., Kostelecký V. A. and Lane C. D.: Phys. Rev. Lett. **85**, 5038-5041 (2000); **89**, 209902-1 (2002).
- [10] Rubin S. M., Spence M. M., Pines A. and Wemmer D. E.: J. Magn. Reson. **152**, 79-86 (2001).
- [11] Verhulst A. S., Liivak O., Sherwood M. H., Vieth H. M. and Chuang I. L.: Appl. Phys. Lett. **79**, 2480-2482 (2001).
- [12] Driehuys B., Cates G. D., Happer W., Mabuchi H., Saam B., Albert M. S. and Wishnia A.: Phys. Lett., A **184**, 88-92 (1993).
- [13] Long H. W., Gaede H. C., Shore J., Reven L., Bowers C. R., Kritzenberger J., Pietrass T., Pines A., Tang P. and Reimer J. A.: J. Am. Chem. Soc. **115**, 8491-8492 (1993).
- [14] Sun X., Hu H. and Zeng X.: Appl. Magn. Reson. **16**, 363-372 (1999).
- [15] Bloembergen N., Pound R. V.: Phys. Rev. **95**, 8-12 (1954).
- [16] Bloom S.: J. Appl. Phys. **28**, 800-805 (1957).
- [17] Szoeké A. and Meiboom S.: Phys. Rev. **113**, 585-586 (1959).
- [18] Bruce C. R., Norberg R. E. and Pake G. E.: Phys. Rev. **104**, 419-420 (1956).
- [19] Abragam A.: The Principles of Nuclear Magnetism, p. 264. Oxford: Clarendon Press 1961.
- [20] Warren W. S., Hames S. L. and Bates J. L.: J. Chem. Phys. **91**, 5895-5904 (1989).
- [21] Jeener J., Vlassenbroek A. and Broekaert P.: J. Chem. Phys. **103**, 1309-1332 (1995).
- [22] Vlassenbroek A., Jeener J. and Broekaert P.: J. Chem. Phys. **103**, 5886-5897 (1995).
- [23] Mao X. A., Wu D. and Ye C. H.: Chem. Phys. Lett. **204**, 123-127 (1993).
- [24] Mao X. A. and Ye C. H.: J. Chem. Phys. **99**, 7455-7462 (1993).
- [25] Mao X. A., Guo J. X. and Ye C. H.: Phys. Rev. B **49**, 15702-15711 (1994).
- [26] Guo J. X. and Mao X. A.: J. Phys. II France **6**, 1183-1193 (1996).
- [27] Chen J. H., Mao X. A. and Ye C. H.: J. Magn. Reson. A **123**, 126-130 (1996).
- [28] Chen J. H., Mao X. A. and Ye C. H.: J. Magn. Reson. **124**, 490-494 (1997).
- [29] Chen J. H. and Mao X. A.: Chem. Phys. Lett. **274**, 549-553 (1997).
- [30] Mao X. A., Guo J. X. and Ye C. H.: Chem. Phys. Lett. **222**, 417-421 (1994).
- [31] Berthault P., Desvaux H., Goff G. L. and Pétro M.: Chem. Phys. Lett. **314**, 52-56 (1999).

- [32] Warren W. S., Richter W., Andreotti A. H. and Farmer II B. T.: Science **262**, 2005-2009 (1993).
- [33] Jeener J.: Phys. Rev. Lett. **82**, 1772-1775 (1999).
- [34] Sauer K. L., Marion F., Nacher P. J. and Tastevin G.: Phys. Rev. B **63**, 184427-1-184427-4 (2001).
- [35] Zhou J., Susumui M., Peter C. M. van Zijl: Magn. Reson. Med. **40**, 712-719 (1998)
- [36] Wong G. P. *et al.*: J. Magn. Reson. **141**, 217-227 (1999).
- [37] Gentile T. R., Rich D. R., Thompson A. K., Snow W. M. and Jones G. L.: J. Res. Natl. Inst. Stand. Technol. **106**, 709-729 (2001).
- [38] Wong-Foy A. *et al.*: J. Magn. Reson. **157**, 235-241 (2002).
- [39] Rosenberry M. A. and Chupp T. E.: Phys. Rev. Lett. **86**, 22-25 (2001).
- [40] Verhulst A. S., Liivak O., Sherwood M. H. and Chung I. L.: J. Magn. Reson. **155**, 145-149 (2002).
- [41] Zeng X., Wu Z., Call T., Miron E., Schreiber D. and Happer W.: Phys. Rev. A **31**, 260-278 (1985).
- [42] Moschos A. and Reisse J.: J. Magn. Reson. **95**, 603-606 (1991).
- [43] Stith A. *et al.*: J. Magn. Reson. **139**, 225-231 (1999).
- [44] Zhou X., Luo J., Sun X., Zeng X., Liu M. and Liu W.: Acta Physica Sinica (*in Chinese*) **51**, 2221-2224 (2002).

Figure captions

Fig. 1 The diagram of our experimental apparatus.

Fig. 2 The experimental ^{129}Xe FID signals that the liquid phase and the solid phase co-existed with radiation damping when the 160° [(a)] pulse was applied and the corresponding frequency spectrum [(b)].

Fig. 3 The experimental liquid phase ^{129}Xe FID signals when 60° [(a1)], 90° [(a2)], 120° [(a3)] and 150° [(a4)] pulses were applied and the corresponding frequency spectra [tagged with (b1,b2,b3,b4)], respectively.

Fig. 4 The envelope of FID with different flip angles under strong radiation damping [(a)]. The theoretical lineshape of water strong radiation damping with the 150° flip pulse excitation, in which the T_{rd} of water proton was assumed to be 12ms[(b)].

Fig. 5 The theoretically simulated ^{129}Xe FID [(a)] and corresponding frequency spectrum [(b)] when the 150° pulse was applied with $T_2^*=30\text{ms}$, and $T_{rd}=5\text{ms}$.

Fig. 6 The theoretical envelopes of the ^{129}Xe FID in the presence of relaxation ($T_2^*=30\text{ms}$) and radiation damping while the different pulse flip angles and T_{rd} were assumed: $T_{rd}=60\text{ms}$ [(a)], $T_{rd}=30\text{ms}$ [(b)], $T_{rd}=15\text{ms}$ [(c)], and $T_{rd}=5\text{ms}$ [(d)].

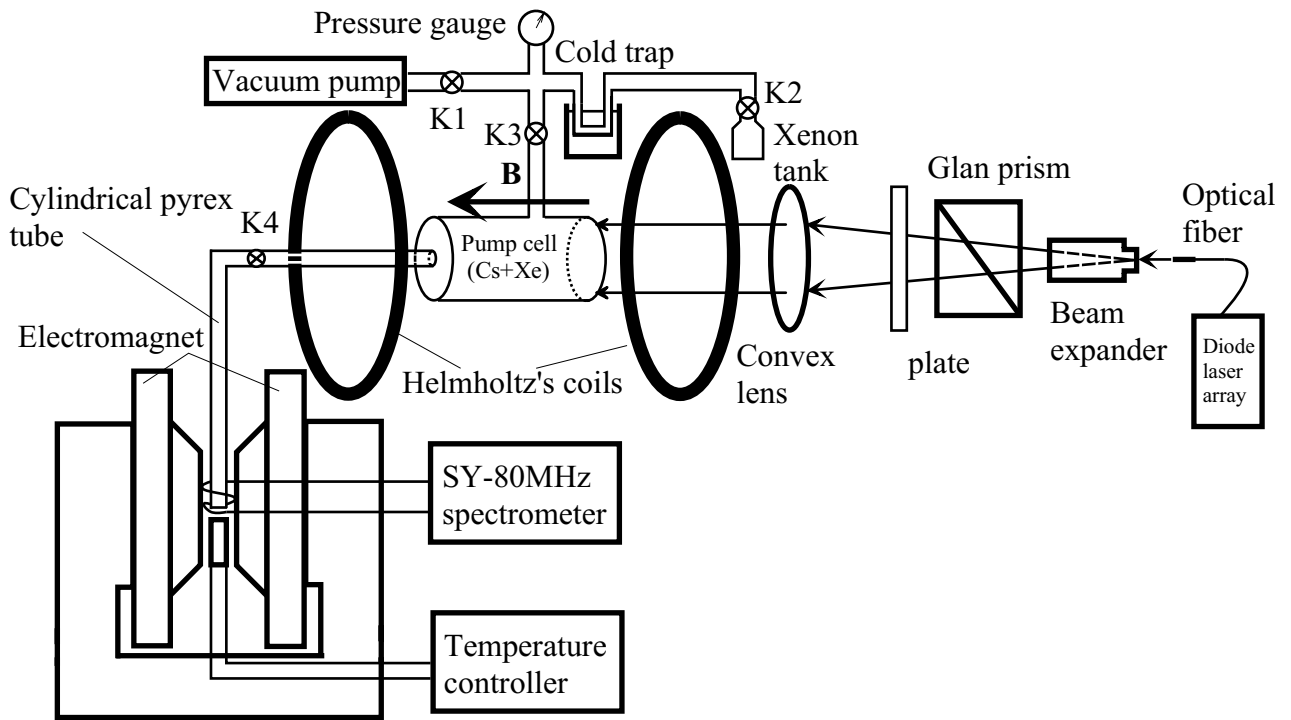


Figure 1

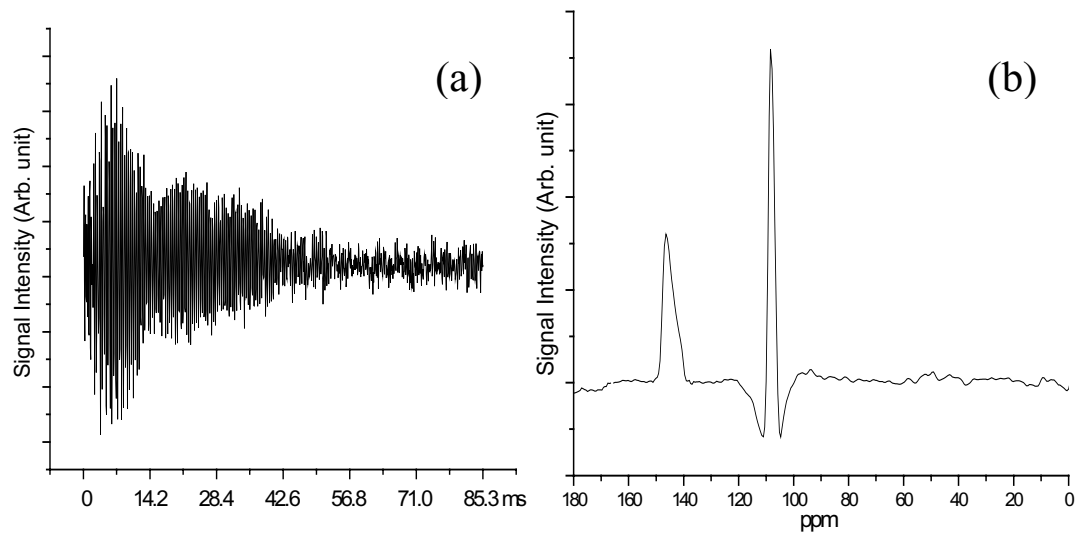


Figure 2

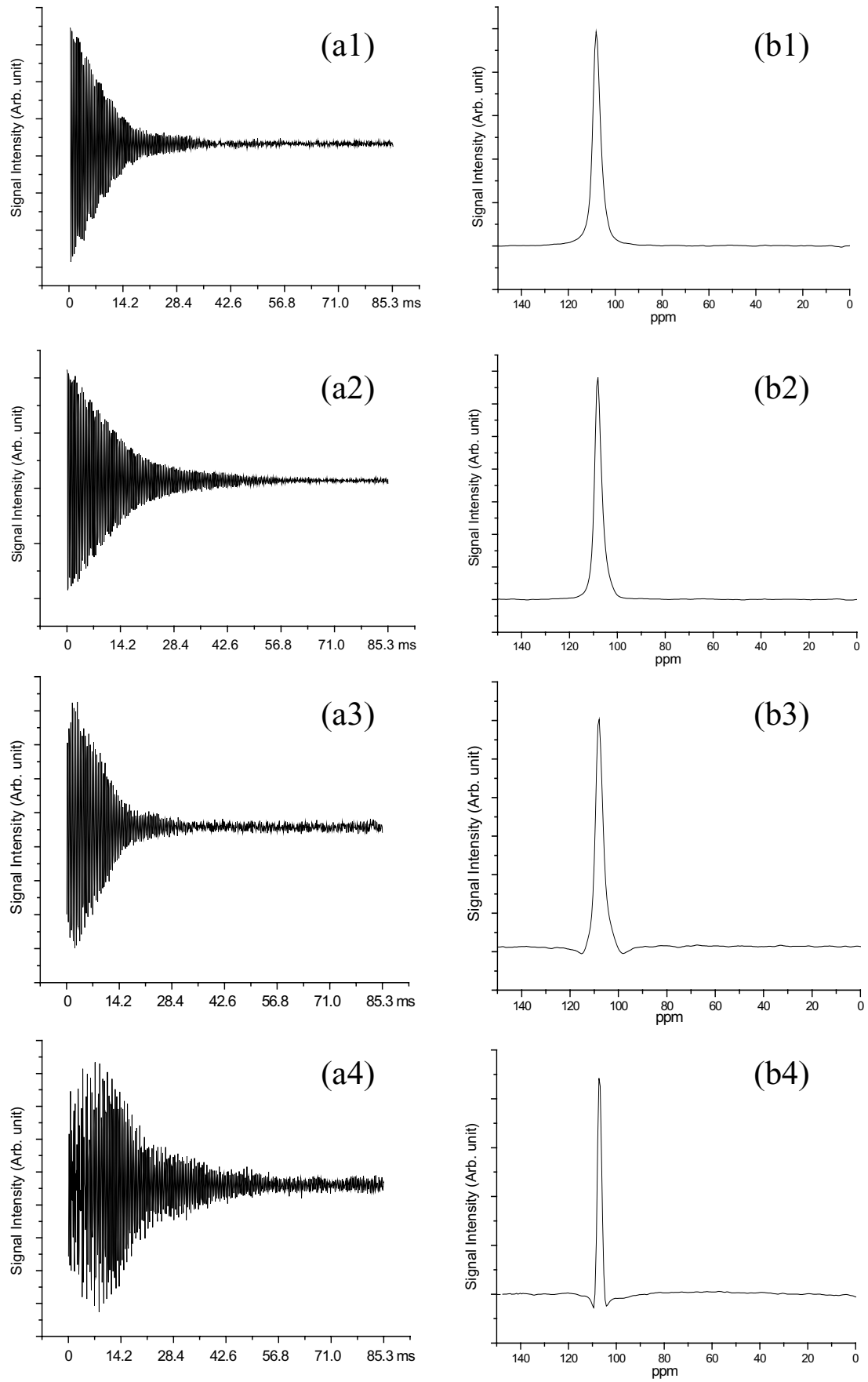


Figure 3

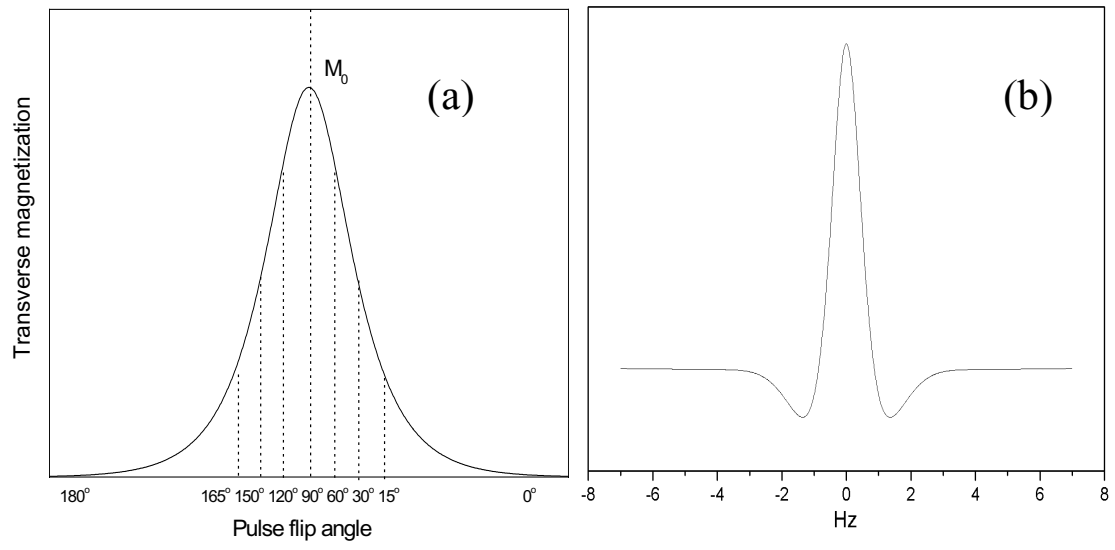


Figure 4

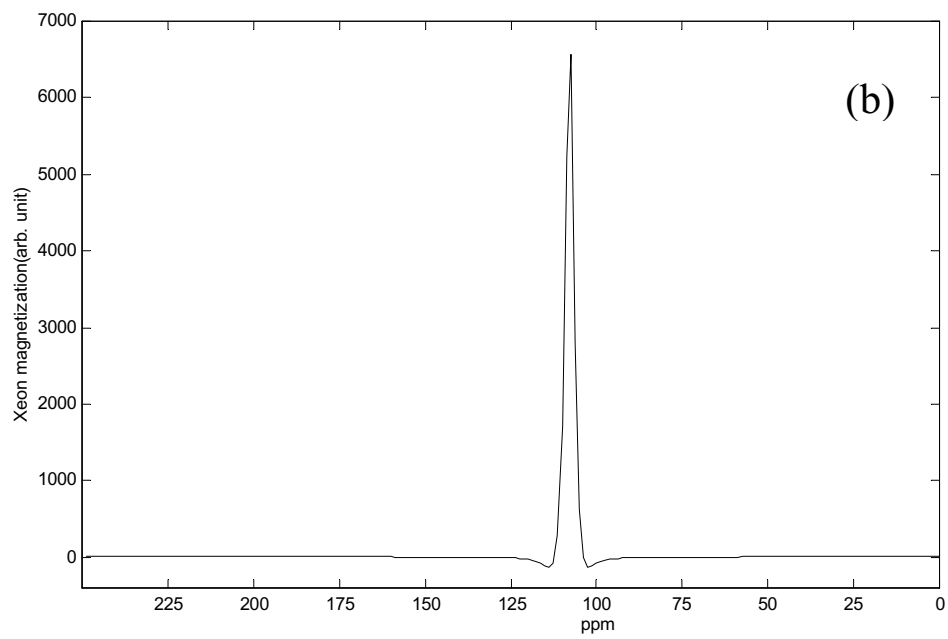
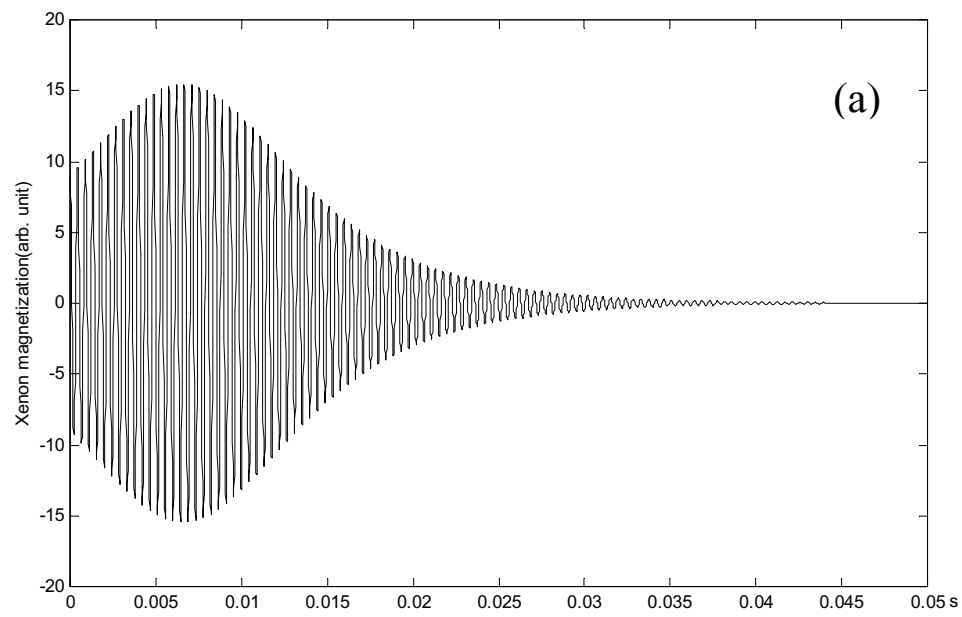


Figure 5

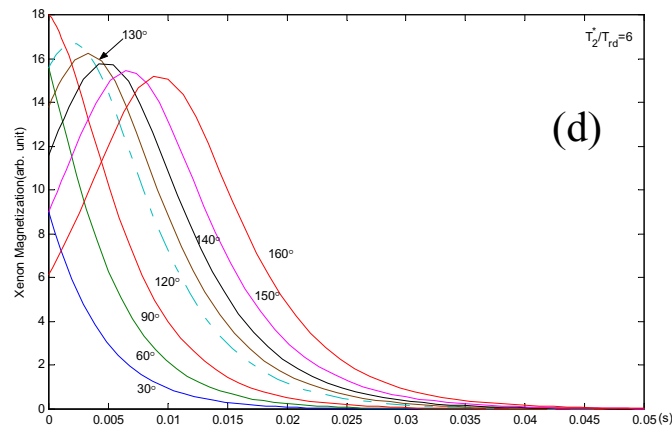
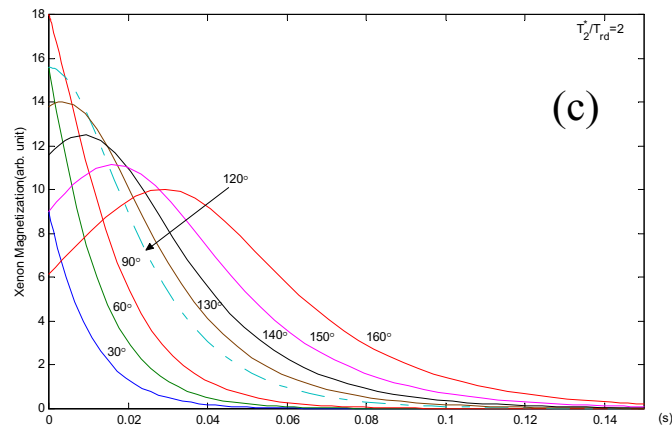
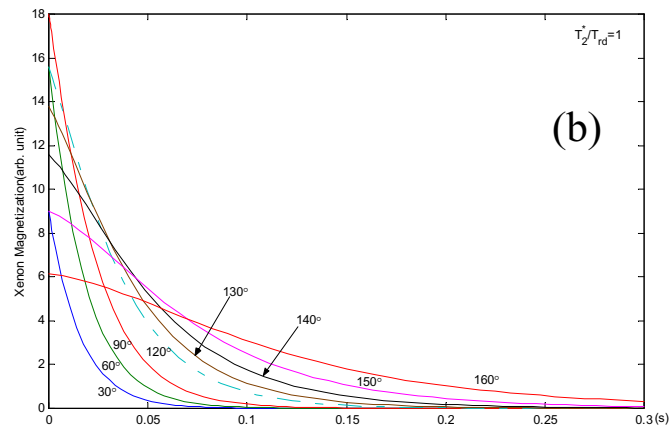
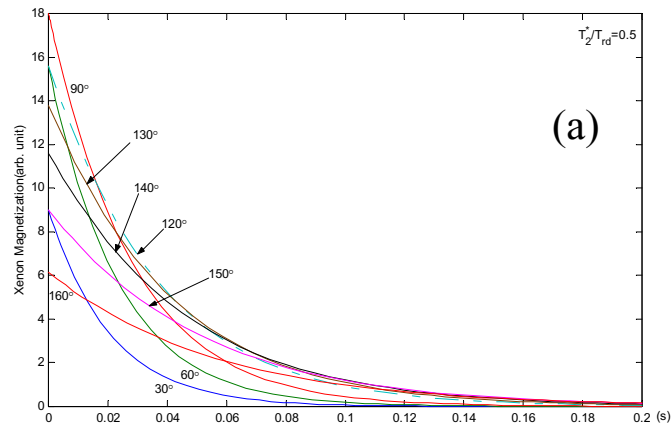


Figure 6